Next generation magnetic nanocomposites: cytotoxic and genotoxic effects of coated and uncoated ferric cobalt boron (FeCoB) nanoparticles in vitro

Running title: cytotoxic and genotoxic effects of coated and uncoated FeCoB nanoparticles in vitro

Katharina Netzer, MD[1]*, Galateja Jordakieva, MD[2]*, Angelika M. Girard, M.Sc.[1], Alexandra C. Budinsky[2], Alexander Pilger, DI[2], Lukas Richter, DI Dr.[3], Nadezhda Kataeva, Dr.[4], Joerg Schotter, Dr.[4], Jasminka Godnic-Cvar, MD[2], Peter Ertl, DI Dr. phil.[5]

[1] Institute of Occupational Medicine, Department of Internal Medicine II, Medical University of Vienna, Währinger Gürtel 18-20, A-1090 Vienna, Austria; Tel.: +43 1 40400 47000

[2] Department of Physical Medicine, Rehabilitation and Occupational Medicine, Medical University of Vienna, Währinger Gürtel 18-20, A-1090 Vienna, Austria; Tel.: +43 1 40400 23080

[3] Siemens Healthcare GmbH, Strategy and Innovation Technology Centre In-Vitro DX & Bioscience, Henkestraße 127, 91052 Erlangen, Germany; Tel.: +49 800 1881885

[4] AIT Austrian Institute of Technology GmbH, Centre for Health & Bioresources, Molecular Diagnostics, Donau-City-Straße 1, 1220 Vienna, Austria; Tel.: +43 (0) 50 5500

[5] Faculty of Technical Chemistry, Vienna University of Technology, Getreidemarkt 9, A-1060 Vienna, Austria; Tel.: +43 1 58801 15001

*contributed equally

Disclosure

All authors state that there are no competing interests regarding this article.

Corresponding Author: Katharina Netzer

E-Mail: katharina.klien@gmx.at

Währinger Gürtel 18-20, Vienna, Austria

Tel: +43 1 40400 47000; Fax: +43 1 4088 011

Abstract

Metal nanoparticles (NPs) have unique physicochemical properties and a widespread application scope depending on their composition and surface characteristics. Potential biomedical applications and the growing diversity of novel nanocomposites highlight the need for toxicological hazard assessment of next generation magnetic nanomaterials. Our study aimed to evaluate the cytotoxic and genotoxic properties of coated and uncoated ferric cobalt boron (FeCoB) NPs (5-15 nm particle size) in cultured human dermal fibroblasts (NHDFs). Cell proliferation was assessed via ATP bioluminescence kit, DNA breakage and chromosomal damage were measured by alkaline comet assay and micronucleus test.

Polyacryl acid-coated FeCoB NPs (PAA-FeCoB NPs) and uncoated FeCoB NPs inhibited cell proliferation at 10 µg ml-1. DNA strand breaks were significantly increased by PAA-coated FeCoB NPs, uncoated FeCoB NPs and l-cysteine-coated FeCoB NPs (Cys-FeCoB NPs), although high concentrations (10 µg ml-1) of coated NPs (Cys- and PAA-FeCoB NPs) showed significantly more DNA breakage when compared to uncoated ones. Uncoated FeCoB NPs and coated NPs (PAA-FeCoB NPs) also induced the formation of micronuclei. Additionally, PAA coated NPs and uncoated FeCoB NPs showed a negative correlation between cell proliferation and DNA strand breaks, suggesting a common pathomechanism, possibly by oxidation induced DNA damage.

We conclude that uncoated FeCoB NPs are cytotoxic and genotoxic at *in vitro* conditions. Surface coating of FeCoB NPs with Cys and PAA does not prevent but rather aggravates DNA damage. Further safety assessment and a well-considered choice of surface coating are needed prior to application of FeCoB nanocomposites in biomedicine.

Keywords: *FeCoB, magnetic nanoparticles, chromosomal damage, DNA damage, next generation nanomaterials, surface coatings*

1 **Introduction and Background**

2   Over the past decades, engineered nanomaterials (NMs) have been used to enhance products

3 with certain desired characteristics in a growing diversity of fields, including construction,

4 electronics and health care (1). Particularly metal NMs with magnetic properties are increasingly

5 designed for biomedical applications in nanomedicine, such as cell separation, drug delivery,

6 hyperthermia and diagnostic resonance imaging, using specific surface coatings to optimise particle

7 stability, solubility and targeting properties. (2)

8 Potential toxicological properties of synthetic nanocomposites, however, are raising safety and

9 health considerations in regards to human and environmental exposure. Since even materials that

10 are known to be chemically inert can be reactive at nanoscale size, (3) it is assumed that the

11 heightened reactivity of NMs may cause adverse health effects. (4) This has been supported by

12 previous *in vitro* and *in vivo* studies showing that nanoparticles (NPs) may induce cytotoxicity,

13 genotoxicity, oxidative stress and inflammation in various human cell lines and animals. (5-10)

14 Interaction of NPs with mammalian cells depends on the size as well as the chemical and physical

15 properties of the respective particle. (11) Surface characteristics of NPs, like surface coating, are

16 also decisive for toxicity. (12, 13) (10.1016/j.toxlet.2017.02.010) Previous studies have

17 demonstrated that NPs can cause cell damage directly by passing through the cell membrane, or

18 indirectly by inducing reactive oxygen species (ROS) or inflammation.(7, 14) Once intracellular,

19 given their small particle size, NPs may gain access to the cellular nucleus either by diffusion,

20 across nuclear pore complexes or by chance. (15-18) Once inside the nucleus, direct interaction

21 between NPs and DNA molecules or DNA related proteins can lead to physical damage of the

22 genetic material. The currently available literature presents partially inconsistent results on

23 cytotoxicity and genotoxicity of NPs, possibly due to a lack of standardised study methods in the

24 past and the enormous variety of engineered NMs. (14) Future studies have yet to determine

25 whether NPs in general or specific physicochemical features of NPs are harmful to humans and the

26 environment. (19, 20)

27   Although the benefits of applying next generation magnetic NM for biomedical purposes are

28   clearly established, the reactivity of nano-carriers and their surface coatings may lead to adverse

29   health effects in resident tissues.(4) Assessment of interactions between different nanocomposites

30   and biological entities could contribute to a safer design of NM, (21) since even coated nontoxic

31   gold nanoparticles have been shown to disrupt intracellular pathways and induce higher

32   susceptibility to apoptotic stimuli in human myocytes. (10.1016/j.tiv.2015.02.010) FeCoB NPs are

33   currently evaluated for use in the electronic industry as magnetic shielding materials, e.g. in

34   microwave absorbers and computer memory compounds. (22, 23) Due to their magnetic properties,

35   FeCoB NPs are also potential next generation NMs candidates for use in nanomedicine. Provided

36   compatible surface coatings to ensure stability and solubility *in vivo*, such as polyacrylic acid

37   (PAA) and l-cysteine (Cys), (24, 25) applications in targeted drug delivery and resonance imaging

38   are feasible. In regard to biomedical applications recent research on cobalt ferrite (CoFe) NPs

39   (10.1016/j.msec.2012.09.003) indicates a cytotoxic and genotoxic potential in human and animal

40   cell   lines   *in   vitro*   (doi.org/10.1007/s1201)(10.1021/acs.chemrestox.6b00377)

41   (10.1371/journal.pone.0168727), however, little is known about the specific toxicity of coated and

42   uncoated FeCoB NPs to human cells.

43   The primary objective of this study was to investigate whether FeCoB NPs induce cytotoxic

44   and genotoxic damages in normal human dermal fibroblasts (NHDFs) to 5-15 nm ferric cobalt

45   boron (FeCoB) NPs at increasing concentrations. The second objective aimed to investigate

46   whether Cys and PAA as surface coatings can modulate any observed cytotoxic and genotoxic

47   effects of FeCoB NPs.

48

49   **Materials and Methods**

50   *Nanoparticle synthesis and preparation of nanoparticle suspensions*

51   Ferric(II) sulphate heptahydrate ($FeSO_4 \cdot 7H_2O$), cobalt(II) chloride hexahydrate ($CoCl_2 \cdot 6H_2O$ 98%),

52   sodium borohydride ($NaBH_4$ 97%), formic acid (HCOOH), dioctyl sulfosuccinate sodium salt

53   (AOT), (1-hexadecyl)trimethylammonium bromid (CTAB), polyacrylic acid 25 wt% solution in

54   water (PAA), L-cysteine 98% and toluene are purchased from Alfa Aesar. Methanol, chloroform,

55   hexane and acetone are obtained from Sigma-Aldrich. All the chemicals are used as received

56   without further purification. Distilled water is used throughout.

57   Three FeCoB NP types (uncoated FeCoB NPs, PAA-coated FeCoB NPs and Cys-coated FeCoB

58   NPs) were synthesised from a two-phase system consisting of water and an organic solvent

59   (hexane) (26-29) The concentration of additionally added surfactants determines the size of the

60   water micelles within the organic solvent. As surfactant, dioctyl sulfosuccinate sodium salt (AOT),

61   [1-Hexadecyl]-trimethyl-ammonium-bromide [CTAB] and dodecylbenzenesulfonic acid sodium

62   salt (DBSNa) are employed at a concentration of 0.3 M. Initially, two separate emulsions containing

63   the metal salts ($FeSO_4$ and $CoCl_2$, 0.3 M, emulsion A) and the reducing agent ($NaBH_4$, 0.6 M,

64   emulsion B) are prepared. Next, the synthesis is initialised by adding emulsion B drop by drop to

65   emulsion A under vigorous stirring at room temperature. When micelles of both solutions combine,

66   microreactors are formed that allow the reduction of the metal salts. Core-shell type nanoparticles

67   are prepared by adding lyophylic agents (L-cys or PAA) to emulsion A at a concentration of 10-20

68   mM. (30) Next, the synthesised nanoparticles are washed several times by centrifugation or

69   separation with a magnet and resuspension in water, acetone or a 1:1 suspension of chloroform and

70   methanol. Afterwards, the nanoparticles are dried for storage.

71   A stock solution of 10 µg ml^{-1} of each NP type was prepared in the NHDF medium (Promocell) and

72   sonicated for at least 10 minutes in a bath-type sonicator (Sonorex Digital 10P, Bandelin). Cells

73 were aseptically treated with three concentrations each of uncoated and PAA-/Cys-coated FeCoB

74 NPs: $0.1\ \mu g\ ml^{-1}$, $1\ \mu g\ ml^{-1}$ and $10\ \mu g\ ml^{-1}$.

75 ***Characterization of nanoparticle suspension***For characterization of aqueous NP suspensions, NP

76 powder was re-suspended in various solutions in a 15 mL tube (Falcon) at a concentration of 1mg

77 mL^{-1}. The particle suspension was exposed to ultrasonic forces for 20 min in order to obtain small

78 aggregates and to keep particles in a floating state using a Bandelin SONOREX™ Digital 10 P

79 ultrasonic bath. Next, particle suspensions were allowed to rest for either 6 hours or 6 days.

80 Supernatants of former suspensions were removed and applied to gravimetric measurements.

81 Gravimetric measurements were applied in 25 mL glass beakers (Schott), which were dried at

82 120°C. The weight of empty vessels was documented. 5mL of each suspension was transferred into

83 the dried vessels in order to evaporate the aqueous solvent in a 100°C heating chamber. Next,

84 samples were allowed to cool down to room temperature in dried atmosphere until a constant mass

85 could be measured. Finally net weight of dried NP was calculated.

86 Particle size distribution in solvents, either DI water or mammalian cell growth medium, was

87 characterised via diffractive light scattering (DLS) measurements. 1mL of each suspension was

88 applied to a "Küvette" and measured in the NanoZS zetasizer by Malvern. Consequently, we

89 employed transmission electron microscopy (TEM) and electron energy loss spectroscopy (EELS)

90 as well as gravimetric methods to analyse the in-house synthesised colloidal FeCoB-NP solutions

91 using a water/oil microemulsion method.(40)

92 ***Cell culture*** Normal human dermal fibroblasts (NHDF) were purchased from Promocell

93 (Heidelberg, Germany), and routinely cultured in Dulbecco's modified eagle's medium DMEM

94 (GIBCO, Paisley, UK) supplemented with 10% heat-inactivated foetal calf serum (FCS)

95 (Biochrom, Berlin, Germany) without antibiotics for ATP bioluminescence and micronucleus test,

96 and fibroblast growth medium (Promocell) without antibiotics for comet assay. Cells were grown as

97 monolayers (standard conditions) in 175 cm^2 flasks (Falcon, Becton Dickinson, Lincoln Park, NJ)

98   at 37 °C in humidified atmosphere containing 5% CO_2 by seeding 5×10^6 cells in 25 ml of

99   appropriate medium. Upon confluency, cells were split using the sterile method. The old medium

100   was discarded and the cells were washed in 5 ml phosphate buffered saline (PBS, GIBCO, Paisley,

101   UK) for bioluminescence and micronucleus test and HepesBSS (Promocell) for comet assay. 3 ml

102   of trypsin/EDTA solution (GIBCO, Invitrogen, Paisley, UK for bioluminescence and micronucleus

103   test and Promocell for comet assay) were added to detach the cells from the flask. 5 ml medium was

104   pipetted into a 15 ml tube (Falcon) and the detached cell suspension was added. The cells were

105   centrifuged for 5 minutes at 200 g at 25 °C. The supernatant was discarded to remove the

106   trypsin/EDTA and the cells were suspended in fresh medium. The cell suspension was then pipetted

107   into fresh culture flasks with a total of 25 ml medium each and then incubated. Fifth to tenth

108   passage cells were used for all experiments. Cellular viability was assessed routinely by trypan blue

109   exclusion.(31) Only cells exhibiting ≥ 80 % viability were used for the following experiments.

110   ***Cell Proliferation measured by ATP Bioluminescence Kit I***

111   Initially, cell proliferation in the presence of increasing concentrations of FeCoB

112   nanoparticles was investigated using the ATP bioluminescence assay. Cell proliferation is energy

113   dependent and requires ATP. When ATP levels fall under a certain point the cell will die since it no

114   longer has the energy to perform basic functions. During apoptosis the ATP levels in a cell decrease

115   significantly. Therefore, a decline of ATP levels indicates inhibited cell proliferation and cell death

116   while an incline is indicative of cell proliferation. The bioluminescence assay uses luciferase to emit

117   ATP and luciferin. For experiments, 7,500 fibroblasts per well were incubated in 96-well flat

118   bottom well plates (NUNC) with DMEM+10% FCS at 37 °C in a humidified atmosphere

119   containing 5% CO_2. After the pre-incubation period of 24 hours the cells were exposed to 0.1, 1 and

120   10 µg ml^{-1} of the three NP types and incubated for 20 hours at 37 °C in a humidified atmosphere

121   containing 5% CO_2. Quantitative ATP levels of exposed fibroblasts were then analysed by

122   measuring the emitted intensity of light [proportional to ATP levels(32)] by a luminometer (Victor

123   3, Perkin Elmer). For each NP type and concentration 3x96-well plates were used making a total of

124   12 wells per dose treatment (12 repeats). The 96-well plate was measured according to the

125   manufacturer's instruction.

126   ***Genotoxicity***

127   *Alkaline Comet Assay*

128   The comet assay was used to investigate DNA damage in order to assess the genotoxic

129   effects of FeCoB NPs on human fibroblasts. The comet assay, also called single-cell gel

130   electrophoresis assay (SCGE), is very sensitive, fast, and versatile. It measures single- and double-

131   stranded DNA breaks at the level of single cells. When alkaline adapted, as in the present paper, the

132   assay can also be used for the quantification of alkali-labile sites.(33, 34) It has been considered a

133   suitable method for analysing nanoparticle-induced oxidative DNA damage. (35) A suspension of

134   exposed individual cells in a low melting agarose gel is layered over a microscope slide. After the

135   agarose solidifies, the cells are lysed and the DNA is electrophoresed. During the electrophoresis

136   the intact chromosomes hardly move at all. But DNA fragments are smaller and travel further. This

137   results in the typical comet shape with the tail extending toward the anode. The length and the

138   relative fluorescence intensity (percentage of DNA in tail) to the head of the comet are measured. It

139   is directly proportional to the level of DNA damage. (34, 36) The experiment for detection of DNA

140   breakage was performed with 50,000 NHDFs, which were exposed to 0.1, 1 and 10 µg ml^{-1} of the

141   three NP types for 48 hours. After lapse of the exposure time cells were washed, trypsinised and

142   suspended in low melting point agarose (purchased from Invitrogen life technologies, Spain) and

143   cased on glass slides with normal melting agarose (purchased from Invitrogen life technologies,

144   Spain). When the first mentioned agarose was solidified the glass slides were suspended in freshly

145   prepared and pre-cooled cell lysis solution for at least one hour at 4 °C. Following, electrophoresis

146   was conducted in alkaline electrophoresis buffer for 20 minutes (conditions: 300 mA, 24 V/cm at 4

147   °C). After completion of the electrophoresis run time the slides were treated with neutralization

148   buffer twice for 8 minutes. The slides were air-dried for 12 to 24 hours at room temperature to let

149   them dry completely until stained with ethidium bromide (Sigma) and examined by fluorescence

150   microscopy at 250 x magnification. Image analysis was performed using 'Comet Assay IV' software

151   (Perspective Instruments, UK) and Axiophot fluorescence microscope (NIKON Japan 520490)

152   attached to a Stingray camera (Allied Vision Technologies, Newburyport, MA, USA). The software

153   automatically calculated values of the tail intensity. All experiments were carried out at least two

154   times in duplicate.

155   *Micronucleus Test*

156   As a second and completing genotoxicity test we have chosen the micronucleus test for the

157   detection of micronuclei (MN) in the cytoplasm of interphase fibroblasts where they may originate

158   as an erratic (third) nucleus from acentric chromosome fragments which is not carried to the poles

159   during the anaphase stage of cell division.

160   Micronuclei are particles that contain chromatin. They are completely separated from the nucleus

161   and are located in the cytoplasm.(37) The formation of a micronucleus (MN) happens during

162   mitosis (metaphase/anaphase transition). The cause of a micronucleus can be either a whole

163   chromosome that was not pulled into one of the newly forming nuclei or an acentric chromosome

164   fragment. 30,000 NHDFs per slide flask were incubated with DMEM+10% FCS at 37 °C in a

165   humidified atmosphere containing 5% CO_2. After the incubation period of 4 hours the cells were

166   incubated with the three NP types at the concentrations of 0.1, 1 and 10 µg ml^{-1} for 72 hours at 37

167   °C in a humidified atmosphere containing 5% CO_2. After 72 hours incubation the cells were fixed

168   and analysed according to Fenech et al. (1985). Micronuclei, defined as rounded bodies, no more

169   than one-third the size of the nucleus, having staining colour and intensity identical to the staining

170   of nuclei, and completely detached from nuclei(38), were scored in up to 2,000 binucleate cells. The

171   data for the two samples from the NP concentrations were pooled. The total MN score per 2,000

172   binucleate cells were calculated.

173   **Statistical Analysis**

174   Additionally to the three toxicity tests described above, statistical correlations between cyto-

175   and genotoxicity were conducted in order to analyse their interrelationship and possible causal

176   mechanisms in cell and DNA damage.

177   Analysis was performed applying the statistical package SPSS 20.0 (SPSS, Chicago, IL). A

178   probability value <0.05 was considered as statistically significant. Continuous variables are

179   expressed as median and range if the assumption of a normal distribution is violated. Groups are

180   compared by Student's t-test or Mann Whitney U test, and the Kruskal-Wallis (H) test as

181   appropriate. Cell proliferation, tail intensity and MN were examined as a continuous variable.

182   Correlation was calculated by the non-parametric Spearman Rho.

183   **Results**

184   The actual size, structure and composition of employed magnetic nanoparticles had to be

185   first determined prior to estimating their toxicity on cell cultures. Although often overlooked in

186   nanotoxicological research, the determination of material characteristics is crucial for a sound

187   understanding of NP interaction with medium components and biological substances, such as

188   proteins and cells.(39) It is important to note that due to the absence of accredited reference

189   nanomaterials for FeCoB-based magnetic nanomaterials and the limited information provided by

190   manufacturing industry regarding synthesis routes and detergents used to stabilize the nanoparticle

191   suspensions, in-house synthesised FeCoB nanoparticle suspensions were used to provide

192   information on nanomaterial size, size distribution, agglomeration state and surface charges. Results

193   of TEM analysis revealed that FeCoB nanoparticles are of spherical shape and consist of a core-

194   shell structure of approx. 8 nm outer diameter (see Fig. 1a, b). As Fe and Co are distributed evenly

195   while B is mostly present in the nanoparticle cores (see EELS analysis in Figure 2), the NP shell is

196   most likely composed of $FeOOH$ and $Co(OH)_2$ groups due to oxidation caused by NP storage at

197   ambient air. The assumption of a core-shell structure of the CoFeB nanoparticles is further

198   supported by EELS spectra taken across a larger area of agglomerated particles. From the spectra

199   (not shown), an atomic composition of the elements Co, Fe and B of 34:36:10 % is deduced. While

200   the content of iron and Co is identical within the accuracy of the measurement, the boron content is

201   reduced due to the depletion of this element in the shell of the nanoparticles.

202   Gravimetric analysis of the uncoated and coated FeCoB nanoparticle suspensions showed

203   that in the absence of stabilizing agents rapid settling of large agglomerates occurred within 30 min.

204   However, after 6 hours resting period a stable NP suspension containing a concentration of

205   approximately 300 µg ml^{-1} for all three types of particles was obtained. Additional stability testing

206   (data not shown) revealed nearly unchanged concentrations of coated and uncoated FeCoB

207   nanoparticles over a period of six days in mammalian cell culture media.

208   Next, agglomeration status, measured by electron microscopy and DLS measurements of the

209   three FeCoB NPs re-suspended in DI water were investigated. Results of the DLS analysis show

210   similar averaged size of agglomerates of 210 nm for PAA coated and 190 nm for uncoated FeCoB

211   NPs in DI water. TEM analysis (data not shown) revealed sizes of single domains in the range of 8-

212   15nm. Interestingly, PAA-coated and Cys-coated FeCoB NP mass showed high fractions of

213   agglomerates (in %) above 750 nm in DI water. However, in the presence of 50 µg mL^{-1} buffered

214   BSA solution averaged sizes of FeCoB-PAA and FeCoB-Cys agglomerates dropped to approx. 210

215   nm and an accompanying change in surface charge was observed, both pointing at a corona effect

216   by physic-chemical adsorption of BSA to the nanoparticles' surface. (41)

Cell Proliferation measured by ATP Bioluminescence KIT

218   As shown in table 1, the exposure of NHDFs to uncoated FeCoB NPs as well as PAA-

219   FeCoB NPs caused a concentration dependent, statistically significant decrease in cell proliferation

220   (p = 0.020, p = 0.035, respectively) while Cys-FeCoB NPs did not. A comparison between the NP

221   types showed a statistically significant difference in cell proliferation at the highest concentration of

222   10 µg ml^{-1} only (p = 0.031).

223   Incubation with 10 µg ml^{-1} PAA-FeCoB NPs induced a significant decrease in cell proliferation

224   when compared to the negative control (p = 0.01) and the medium concentration of 1 µg ml^{-1} (p =

225   0.029). Uncoated FeCoB NPs caused a significant inhibition of cell proliferation at 10 µg ml^{-1}

226   compared with the negative control (p = 0.01) as well as the lowest concentration of 0.1 µg ml^{-1} (p

227   = 0.029).

Genotoxicity

Alkaline Comet Assay

230   As shown in table 2, all three investigated NPs (FeCoB, PAA-FeCoB, Cys-FeCoB) caused a

231   concentration dependent increase in DNA strand breaks (p = 0.016, p = 0.002, p = 0.011,

232 respectively). A comparison between the NP types showed a significant difference in DNA strand

233 breaks at the concentrations of 1 µg ml^{-1} and 10 µg ml^{-1} (p = 0.032, p = 0.012, respectively).

234 At 10 µg ml^{-1} all three NP types (FeCoB, PAA-FeCoB, Cys-FeCoB) induced significantly more

235 DNA breakage when compared to the negative control (p = 0.002, p = 0.001 and p = 0.001,

236 respectively) and to the lowest concentration of 0.1 µg ml^{-1} (p = 0.029, p = 0.002 and p = 0.002,

237 respectively). The exposure to 1 µg ml^{-1} of both kinds of coated NPs (PAA-FeCoB and Cys-

238 FeCoB) resulted in a significant increase of DNA breakage (p = 0.009 and p = 0.001) as compared

239 to the negative control.

240 Finally, 10 µg ml^{-1} of coated NPs (PAA-FeCoB and Cys-FeCoB) induced more DNA strand breaks

241 than the uncoated NPs (FeCoB) at the same concentration (p = 0.01 both).

242 *Micronucleus Test*

243   A concentration dependent increase in the frequency of micronuclei (MN) was induced by

244 uncoated FeCoB and PAA-FeCoB (p = 0.002 and p = 0.001, respectively) (Table 3). NHDFs treated

245 with 10 µg ml^{-1} of uncoated FeCoB and PAA-FeCoB showed significantly higher levels of MN

246 when compared to the negative control (p = 0.008 and p = 0.04, respectively), to 0.1 µg ml^{-1} (p =

247 0.000, both) and 1 µg ml^{-1} (p = 0.021 and p =0.004, respectively). Significant differences were also

248 observed between the negative control and 0.1 µg ml^{-1} Cys-FeCoB NPs. Interestingly, 0.1 µg ml^{-1}

249 Cys-FeCoB did show lower levels of MN compared to the negative control.

250   A low negative correlation (r = -0.499, p = 0.001) was observed between the DNA damages

251 assessed by the comet assay and the inhibition of cell proliferation assessed by the ATP

252 bioluminescence kit. Considering uncoated FeCoB NPs separately, we found a moderate negative

253 correlation (r = -0.650, p = 0.022) between comet assay and cell proliferation. Similarly, PAA-

254 coated FeCoB NPs revealed a very strong negative correlation (r = -0.832, p = 0.001) between

255 comet assay and cell proliferation.

256

257   **Discussion**

258   The aim of this study was to investigate whether FeCoB NPs are cytotoxic and genotoxic to human

259   dermal fibroblasts (NHDFs) and further if surface characteristics, namely Cys- and PAA-coatings

260   can modulate any observed effects. To our knowledge, this is the first study to address the

261   toxicological properties of these specific nanocomposites.

262   Primary cell cultures were used in this study because they are more likely to display natural

263   phenotypes, thus mimicking *in vivo* situations.(42) Human fibroblasts represent excellent indicator

264   cells for nanotoxicological studies as they are spread throughout the human body and secure the

265   integrity of soft connective tissue by producing various components of the extracellular matrix, e.g.

266   collagen and fibronectin fibres. Thereby, fibroblasts are indispensable for biological processes such

267   as wound healing, immunological reactions, angiogenesis and (re)construction of connective tissue.

268   (43) It has been reported that various human cells including fibroblasts release reactive oxygen

269   species (ROS) in answer to NP exposure which in turn can trigger further pathophysiological effects

270   such as inflammation and genotoxicity.(44)

271   Consistent with prior nanotoxicological studies(5, 45), we observed a clear genotoxic potential

272   of both uncoated (FeCoB) and coated (Cys- and PAA-FeCoB) NPs as evidenced by a concentration

273   dependent increase in DNA and chromosomal damage in exposed fibroblasts. Contrary to our

274   expectations and controversial with some previous studies(46-49), coating of NPs did not prevent

275   their genotoxic and cytotoxic effects. Our experiments showed that Cys- and PAA-coated FeCoB

276   NPs resulted in increased DNA strand breaks at even lower concentrations and apparently caused

277   more DNA breakage when compared to uncoated FeCoB NPs. Sato et al., however, have previously

278   described that coating of NPs with polyethylene glycol (PEG) - a biocompatible polymer - reduces

279   the interaction between the particle itself and serum proteins potentially resulting in an impaired

280   direct particle-cell-interaction.(50) Negatively charged surfaces, on the other hand, such as PAA-

281   coated NPs due to their carboxylic groups (51) seem to increase the particles' affinity to cell

282 membranes to a considerably greater extent than uncoated or neutrally charged NPs.(52) Once

283 inside the fibroblasts, NPs may have facilitated access to the cellular nucleus and the DNA, the site

284 of possible genotoxic damage. The importance of our findings, showing that coated NPs display a

285 rather unexpected higher potential in inducing DNA breakage in fibroblasts, is further emphasised

286 by Ahamed et al. who revealed that polysaccharide coated NPs induce more severe DNA damage in

287 mammalian cells than uncoated NPs. As to the authors this effect can be attributed to the fact that

288 polysaccharide coatings prevent the formation of particle aggregation resulting in a much bigger

289 surface area per particle mass and thus greater contact with membrane bound organelles.(53) Still,

290 future experiments are warranted to examine these biological effects of particle aggregation in more

291 detail. In summary, fibroblasts showed significant DNA breakage after the exposure to high

292 concentrations (10 µg ml-1) of both uncoated and coated FeCoB NPs although the comparison

293 among particle types clearly revealed a higher genotoxic potential in behalf of the coated NPs.

294   The second genotoxic effect observed in this study was chromosomal damage. According to

295 the micronucleus test, only the highest concentration (10 µg ml^{-1}) of both uncoated FeCoB as well

296 as PAA-coated FeCoB NPs induced the formation of micronuclei (MN) in cultured fibroblasts

297 (Table 3). Previous studies have described an increase of MN formation by various metal NPs both

298 *in vitro*(54, 55) and *in vivo*(56-58), although current literature remains inconsistent at this point in

299 time. Interestingly, Cys-FeCoB NPs did not increase MN formation in our study; on the contrary, it

300 rather appeared as if low concentrations of Cys-FeCoB NPs (0.1 µg ml^{-1}) prevented chromosomal

301 damage (Table 3). Even if comparable genotoxicity studies of Cys-coated NPs are lacking, their

302 cytotoxicity was examined by Hahn et al. The authors observed that cysteine-coated metal NPs

303 inhibited the viability of human coronary artery cells much less than uncoated metal NPs.(59)

304   Numerous studies that demonstrated nanoparticulate genotoxicity also point out that some

305 metal NPs additionally feature cytotoxic potential.(60-62) Generally, metal NPs can be toxic to

306 living cells due to either direct particle-cell interactions or by indirectly releasing metal ions.(59)

307   Our results provide evidence that both uncoated and PAA-coated FeCoB NPs inhibit cell

308   proliferation in NHDFs whereas the cysteine-coated particles seemed to be non-cytotoxic as long as

309   concentrations did not exceed 1 µg ml^{-1} (Table 1). As cysteine is known to create metal ion

310   complexes, it is therefore presumable that it reduces cytotoxicity of metals released by NPs at low

311   concentrations. Possibly, particle concentrations above 1 µg ml^{-1} overburden the ability of cysteine

312   to form metal ion complexes. Amongst others(5, 6, 63, 64), the results of Guichard et al.(64) and

313   Srinivas et al.(65) support our observed inhibition of cell proliferation following exposure to high

314   concentrations of uncoated FeCoB NPs. Both study groups demonstrated clear cytotoxic effects of

315   nanoparticulate iron oxide in incubated hamster embryo cells and increased oxidative stress in

316   inhalation exposed rats, respectively.(64)'(65) As for PAA-coated FeCoB NPs, we can speculate

317   that their negatively charged surface - in correspondence to their supposed genotoxic mechanism -

318   might as well be responsible for the herein observed inhibition of cell proliferation. This theory is

319   supported by the results of Wan et al. who showed a definite inhibition in mouse cell viability and

320   cell adhesion as well as destroyed cellular membranes after treatment with PAA-coated iron oxide

321   NPs.(51) Controversial observations have been made by Yin et al. who detected very little

322   cytotoxicity in lymphoblastoid cells following exposure to zinc oxide NPs coated with poly methyl

323   acrylic acid.(66) In reference to comparable experimental conditions such as the similarity in

324   applied NPs, the concordant results of Wan et al.(51) seem to be more appropriate for the

325   interpretation of our results.

326   Finally, the negative correlation between cell proliferation and DNA damage suggests that both

327   uncoated and PAA-coated FeCoB NP follow a common pathomechanism of inhibiting cell

328   proliferation and generating DNA breakage. A plausible mutuality of these two particles might be

329   the induction of oxidative stress. Since oxidative stress together with oxidation-induced DNA strand

330   breaks were frequently observed after the exposure to various NPs(67-69), DNA damages of the

331   herein investigated FeCoB and PAA-FeCoB NPs might eventually be a consequence of oxidative

332   overload. Continuing studies are needed to further investigate the mechanism of their possible

333 indirect DNA damaging potential, e.g. by means of modified comet assays including frequently

334 used base excision repair enzymes to specifically detect oxidation damaged DNA such as oxidised

335 purines.(70) A reasonable explanation for the absent correlation between DNA breakage and

336 chromosomal damage can be the indispensable necessity of nuclear division for MN formation

337 whereas DNA breakage may also occur in its absence.(38) Furthermore, the two applied

338 genotoxicity tests in our study measure different biological endpoints. While the alkaline comet

339 assay measures principally reversible and repairable DNA strand breaks (single and double DNA

340 strand breaks, alkali labile sites), the micronucleus test detects chromosomal mutations (aneuploidy

341 and clastogenicity), which in general are not repairable.(71) A potential limitation of this study is

342 the lack of interference testing, which has recently been recommended for *in vitro* NP experiments.

343 (72-74) However, due to the strong consistency between our micronucleus and visual comet assay

344 findings, a sufficient validity of our results is still to be expected. (75)

345 *Conclusions*

346 Our data provides evidence to the genotoxicity of both uncoated and coated FeCoB NPs. Further,

347 coated NPs (L-Cys- and PAA-coated FeCoB NPs) induced a greater extent of DNA damage than

348 uncoated FeCoB NPs. Based on these findings we assume a larger reactive surface area of coated

349 FeCoB NPs due to the prevention of particle aggregation. In addition PAA-coated FeCoB NPs

350 showed cytotoxic effects, potentially due to their negative surface charge. In light of these initial

351 findings, modifying particle surfaces might be an option to prevent or mitigate suspected cyto- and

352 genotoxic effects. In summary, our study presents additional evidence of the cytotoxic and

353 genotoxic properties of engineered NMs and the significant effect of surface characteristics on

354 toxicity. Composition and coating dependent interactions with biological entities have to be taken

355 into account when considering novel nanomaterials for *in vivo* biomedical applications.

356

357

Acknowledgements

References

1. Mihalache R, Verbeek J, Graczyk H, Murashov V, van Broekhuizen P. Occupational exposure limits for manufactured nanomaterials, a systematic review. Nanotoxicology. 2017:1-13.
2. Colombo M, Carregal-Romero S, Casula MF, Gutierrez L, Morales MP, Bohm IB, et al. Biological applications of magnetic nanoparticles. Chem Soc Rev. 2012;41(11):4306-34.
3. Schrand AM, Rahman MF, Hussain SM, Schlager JJ, Smith DA, Syed AF. Metal-based nanoparticles and their toxicity assessment. Wiley interdisciplinary reviews Nanomedicine and nanobiotechnology. 2010;2(5):544-68.
4. Kaluza S HB, Jankowsky E, Rosell M. Workplace exposure to nanoparticles2009:[89 p.].
5. Papageorgiou I, Brown C, Schins R, Singh S, Newson R, Davis S, et al. The effect of nano- and micron-sized particles of cobalt-chromium alloy on human fibroblasts in vitro. Biomaterials. 2007;28(19):2946-58.
6. Lewinski N, Colvin V, Drezek R. Cytotoxicity of nanoparticles. Small. 2008;4(1):26-49.
7. Iavicoli I, Leso V, Fontana L, Bergamaschi A. Toxicological effects of titanium dioxide nanoparticles: a review of in vitro mammalian studies. European review for medical and pharmacological sciences. 2011;15(5):481-508.
8. Nel A, Xia T, Madler L, Li N. Toxic potential of materials at the nanolevel. Science. 2006;311(5761):622-7.
9. Sayes CM, Reed KL, Warheit DB. Assessing toxicity of fine and nanoparticles: comparing in vitro measurements to in vivo pulmonary toxicity profiles. Toxicological sciences : an official journal of the Society of Toxicology. 2007;97(1):163-80.
10. Xia T, Kovochich M, Brant J, Hotze M, Sempf J, Oberley T, et al. Comparison of the abilities of ambient and manufactured nanoparticles to induce cellular toxicity according to an oxidative stress paradigm. Nano letters. 2006;6(8):1794-807.
11. Verma A, Stellacci F. Effect of surface properties on nanoparticle-cell interactions. Small. 2010;6(1):12-21.
12. Warheit DB, Reed KL, Sayes CM. A role for nanoparticle surface reactivity in facilitating pulmonary toxicity and development of a base set of hazard assays as a component of nanoparticle risk management. Inhalation toxicology. 2009;21 Suppl 1:61-7.
13. Kwok KW, Dong W, Marinakos SM, Liu J, Chilkoti A, Wiesner MR, et al. Silver nanoparticle toxicity is related to coating materials and disruption of sodium concentration regulation. Nanotoxicology. 2016;10(9):1306-17.
14. Singh N, Manshian B, Jenkins GJ, Griffiths SM, Williams PM, Maffeis TG, et al. NanoGenotoxicology: the DNA damaging potential of engineered nanomaterials. Biomaterials. 2009;30(23-24):3891-914.
15. Catalan J, Jarventaus H, Vippola M, Savolainen K, Norppa H. Induction of chromosomal aberrations by carbon nanotubes and titanium dioxide nanoparticles in human lymphocytes in vitro. Nanotoxicology.
16. Tkachenko AG, Xie H, Liu Y, Coleman D, Ryan J, Glomm WR, et al. Cellular trajectories of peptide-modified gold particle complexes: comparison of nuclear localization signals and peptide transduction domains. Bioconjugate chemistry. 2004;15(3):482-90.
17. Oberdorster G, Maynard A, Donaldson K, Castranova V, Fitzpatrick J, Ausman K, et al. Principles for characterizing the potential human health effects from exposure to nanomaterials: elements of a screening strategy. Particle and fibre toxicology. 2005;2:8.
18. Donaldson K, Poland CA. Inhaled nanoparticles and lung cancer - what we can learn from conventional particle toxicology. Swiss Med Wkly.142:w13547.
19. Schwarze PE, Ovrevik J, Lag M, Refsnes M, Nafstad P, Hetland RB, et al. Particulate matter properties and health effects: consistency of epidemiological and toxicological studies. Human & experimental toxicology. 2006;25(10):559-79.
20. Maynard AD. Nanotechnology: the next big thing, or much ado about nothing? The Annals of occupational hygiene. 2007;51(1):1-12.

21.   Rosslein M, Liptrott N, Owen A, Boisseau P, Wick P, Herrmann IK. Sound Understanding of Environmental, Health and Safety, Clinical, and Market Aspects is Imperative to Clinical Translation of Nanomedicines. Nanotoxicology. 2017:1-6.

22.   Luo M, Zhou P, Liu Y, Wang X, Xie J. Electric-Field-Induced Amplitude Tuning of Ferromagnetic Resonance Peak in Nano-granular Film FeCoB-SiO2/PMN-PT Composites. Nanoscale research letters. 2016;11(1):493.

23.   Kim JH, Lee JB, An GG, Yang SM, Chung WS, Park HS, et al. Ultrathin W space layer-enabled thermal stability enhancement in a perpendicular MgO/CoFeB/W/CoFeB/MgO recording frame. Scientific reports. 2015;5:16903.

24.   Lungu, II, Radulescu M, Mogosanu GD, Grumezescu AM. pH sensitive core-shell magnetic nanoparticles for targeted drug delivery in cancer therapy. Romanian journal of morphology and embryology = Revue roumaine de morphologie et embryologie. 2016;57(1):23-32.

25.   Liang S, Zhou Q, Wang M, Zhu Y, Wu Q, Yang X. Water-soluble L-cysteine-coated FePt nanoparticles as dual MRI/CT imaging contrast agent for glioma. International journal of nanomedicine. 2015;10:2325-33.

26.   Ago H, Ohshima S, Uchida K, Yumura M. Gas-phase synthesis of single-wall carbon nanotubes from colloidal solution of metal nanoparticles. J Phys Chem B. 2001;105(43):10453-6.

27.   Chen JP, Lee KM, Sorensen CM, Klabunde KJ, Hadjipanayis GC. Magnetic-Properties of Microemulsion Synthesized Cobalt Fine Particles. J Appl Phys. 1994;75(10):5876-8.

28.   Duarte EL, Itri R, Lima E, Baptista MS, Berquo TS, Goya GF. Large magnetic anisotropy in ferrihydrite nanoparticles synthesized from reverse micelles. Nanotechnology. 2006;17(22):5549-55.

29.   Seip CT, Carpenter EE, O'Connor CJ, John VT, Li SC. Magnetic properties of a series of ferrite nanoparticles synthesized in reverse micelles. Ieee T Magn. 1998;34(4):1111-3.

30.   Huang KC, Ehrman SH. Synthesis of iron nanoparticles via chemical reduction with palladium ion seeds. Langmuir : the ACS journal of surfaces and colloids. 2007;23(3):1419-26.

31.   Strober W. Trypan blue exclusion test of cell viability. Curr Protoc Immunol. 2001;Appendix 3:Appendix 3B.

32.   DeLuca M, McElroy WD. Kinetics of the firefly luciferase catalyzed reactions. Biochemistry. 1974;13(5):921-5.

33.   Pavanello S, Clonfero E. Biological indicators of genotoxic risk and metabolic polymorphisms. Mutation research. 2000;463(3):285-308.

34.   Collins AR, Oscoz AA, Brunborg G, Gaivao I, Giovannelli L, Kruszewski M, et al. The comet assay: topical issues. Mutagenesis. 2008;23(3):143-51.

35.   Pfaller T, Colognato R, Nelissen I, Favilli F, Casals E, Ooms D, et al. The suitability of different cellular in vitro immunotoxicity and genotoxicity methods for the analysis of nanoparticle-induced events. Nanotoxicology. 2010;4(1):52-72.

36.   Tice RR, Agurell E, Anderson D, Burlinson B, Hartmann A, Kobayashi H, et al. Single cell gel/comet assay: guidelines for in vitro and in vivo genetic toxicology testing. Environmental and molecular mutagenesis. 2000;35(3):206-21.

37.   Schiffmann D, De Boni U. Dislocation of chromatin elements in prophase induced by diethylstilbestrol: a novel mechanism by which micronuclei can arise. Mutation research. 1991;246(1):113-22.

38.   Fenech M. The in vitro micronucleus technique. Mutation research. 2000;455(1-2):81-95.

39.   Maynard AD. Nanotechnology: assessing the risks. Nano Today. 2006;1(2):22-33.

40.   Linderoth S, M⊘rup S, Bentzon MD. Influence of pH on the composition and structure of Fe-Co-B alloy particles prepared by borohydride reduction in aqueous solutions. Journal of Magnetism and Magnetic Materials. 1990;83(1–3):457-9.

41.   Salis A, Bostrom M, Medda L, Cugia F, Barse B, Parsons DF, et al. Measurements and Theoretical Interpretation of Points of Zero Charge/Potential of BSA Protein. Langmuir : the ACS journal of surfaces and colloids. 2011;27(18):11597-604.

42.   Kunzmann A, Andersson B, Thurnherr T, Krug H, Scheynius A, Fadeel B. Toxicology of engineered nanomaterials: Focus on biocompatibility, biodistribution and biodegradation. Biochim Biophys Acta. 2010;article in press.

43.   Ruszczak Z. Effect of collagen matrices on dermal wound healing. Advanced Drug Delivery Reviews. 2003;55(12):1595-611.

44.   Manke A, Wang L, Rojanasakul Y. Mechanisms of Nanoparticle-Induced Oxidative Stress and Toxicity. Biomed Res Int. 2013;2013:942916.

45.   Hong SC, Lee JH, Lee J, Kim HY, Park JY, Cho J, et al. Subtle cytotoxicity and genotoxicity differences in superparamagnetic iron oxide nanoparticles coated with various functional groups. International journal of nanomedicine.6:3219-31.

46.   Borm PJ, Robbins D, Haubold S, Kuhlbusch T, Fissan H, Donaldson K, et al. The potential risks of nanomaterials: a review carried out for ECETOC. Particle and fibre toxicology. 2006;3:11.

47.   Hsiao IL, Huang YJ. Titanium oxide shell coatings decrease the cytotoxicity of ZnO nanoparticles. Chemical research in toxicology. 2011;24(3):303-13.

48.   Ai J, Biazar E, Jafarpour M, Montazeri M, Majdi A, Aminifard S, et al. Nanotoxicology and nanoparticle safety in biomedical designs. International journal of nanomedicine. 2011;6:1117-27.

49.   Snyder MA, Lee JA, Davis TM, Scriven LE, Tsapatsis M. Silica nanoparticle crystals and ordered coatings using lys-sil and a novel coating device. Langmuir : the ACS journal of surfaces and colloids. 2007;23(20):9924-8.

50.   Sato A, Choi SW, Hirai M, Yamayoshi A, Moriyama R, Yamano T, et al. Polymer brush-stabilized polyplex for a siRNA carrier with long circulatory half-life. Journal of controlled release : official journal of the Controlled Release Society. 2007;122(3):209-16.

51.   Wan S, Huang J, Guo M, Zhang H, Cao Y, Yan H, et al. Biocompatible superparamagnetic iron oxide nanoparticle dispersions stabilized with poly(ethylene glycol)-oligo(aspartic acid) hybrids. Journal of biomedical materials research Part A. 2007;80(4):946-54.

52.   Wilhelm C, Billotey C, Roger J, Pons JN, Bacri JC, Gazeau F. Intracellular uptake of anionic superparamagnetic nanoparticles as a function of their surface coating. Biomaterials. 2003;24(6):1001-11.

53.   Ahamed M, Karns M, Goodson M, Rowe J, Hussain SM, Schlager JJ, et al. DNA damage response to different surface chemistry of silver nanoparticles in mammalian cells. Toxicology and applied pharmacology. 2008;233(3):404-10.

54.   Shukla RK, Kumar A, Pandey AK, Singh SS, Dhawan A. Titanium dioxide nanoparticles induce oxidative stress-mediated apoptosis in human keratinocyte cells. Journal of biomedical nanotechnology. 2011;7(1):100-1.

55.   Kim YS, Kim JS, Cho HS, Rha DS, Kim JM, Park JD, et al. Twenty-eight-day oral toxicity, genotoxicity, and gender-related tissue distribution of silver nanoparticles in Sprague-Dawley rats. Inhalation toxicology. 2008;20(6):575-83.

56.   Kim HR, Kim MJ, Lee SY, Oh SM, Chung KH. Genotoxic effects of silver nanoparticles stimulated by oxidative stress in human normal bronchial epithelial (BEAS-2B) cells. Mutation research. 2011;726(2):129-35.

57.   Balasubramanyam A, Sailaja N, Mahboob M, Rahman MF, Hussain SM, Grover P. In vivo genotoxicity assessment of aluminium oxide nanomaterials in rat peripheral blood cells using the comet assay and micronucleus test. Mutagenesis. 2009;24(3):245-51.

58.   Trouiller B, Reliene R, Westbrook A, Solaimani P, Schiestl RH. Titanium dioxide nanoparticles induce DNA damage and genetic instability in vivo in mice. Cancer research. 2009;69(22):8784-9.

59.   Hahn A, Fuhlrott J, Loos A, Barcikowski S. Cytotoxicity and ion release of alloy nanoparticles. Journal of nanoparticle research : an interdisciplinary forum for nanoscale science and technology. 2012;14(1):1-10.

60.   Alarifi S, Ali D, Verma A, Alakhtani S, Ali BA. Cytotoxicity and genotoxicity of copper oxide nanoparticles in human skin keratinocytes cells. Int J Toxicol. 2013;32(4):296-307.

61.   Hamzeh M, Sunahara GI. In vitro cytotoxicity and genotoxicity studies of titanium dioxide (TiO2) nanoparticles in Chinese hamster lung fibroblast cells. Toxicol In Vitro. 2013;27(2):864-73.

62.   Shukla RK, Kumar A, Gurbani D, Pandey AK, Singh S, Dhawan A. TiO(2) nanoparticles induce oxidative DNA damage and apoptosis in human liver cells. Nanotoxicology. 2013;7(1):48-60.

63.   Wu J, Sun J. Investigation on mechanism of growth arrest induced by iron oxide nanoparticles in PC12 cells. Journal of nanoscience and nanotechnology. 2011;11(12):11079-83.

64.   Guichard Y, Schmit J, Darne C, Gate L, Goutet M, Rousset D, et al. Cytotoxicity and genotoxicity of nanosized and microsized titanium dioxide and iron oxide particles in Syrian hamster embryo cells. The Annals of occupational hygiene. 2012;56(5):631-44.

65.   Srinivas A, Jaganmohan Rao P, Selvam G, Goparaju A, Balakrishna Murthy P, Neelakanta Reddy P. Oxidative stress and inflammatory responses of rat following acute inhalation exposure to iron oxide nanoparticles. Human & experimental toxicology. 2012.

66.   Yin H, Casey PS, McCall MJ. Surface modifications of ZnO nanoparticles and their cytotoxicity. Journal of nanoscience and nanotechnology. 2010;10(11):7565-70.

67.   Gurr JR, Wang AS, Chen CH, Jan KY. Ultrafine titanium dioxide particles in the absence of photoactivation can induce oxidative damage to human bronchial epithelial cells. Toxicology. 2005;213(1-2):66-73.

68.   Shukla RK, Sharma V, Pandey AK, Singh S, Sultana S, Dhawan A. ROS-mediated genotoxicity induced by titanium dioxide nanoparticles in human epidermal cells. Toxicology in vitro : an international journal published in association with BIBRA. 2011;25(1):231-41.

69.   Sharma V, Singh SK, Anderson D, Tobin DJ, Dhawan A. Zinc oxide nanoparticle induced genotoxicity in primary human epidermal keratinocytes. Journal of nanoscience and nanotechnology. 2011;11(5):3782-8.

70.   Moller P. The alkaline comet assay: towards validation in biomonitoring of DNA damaging exposures. Basic Clin Pharmacol Toxicol. 2006;98(4):336-45.

71.   Van Goethem F, Lison D, Kirsch-Volders M. Comparative evaluation of the in vitro micronucleus test and the alkaline single cell gel electrophoresis assay for the detection of DNA damaging agents: genotoxic effects of cobalt powder, tungsten carbide and cobalt-tungsten carbide. Mutation research. 1997;392(1-2):31-43.

72)   Dekkers et al., 2016. Towards a nanospecific approach for risk assessment. Regulatory Toxicology and Pharmacology 80 (2016) 46-59.

73)   Piret et al., 2016. Pan‑European inter‑laboratory studies on a panel of in vitro cytotoxicity and pro‑inflammation assays for nanoparticles. Arch Toxicol. DOI 10.1007/s00204-016-1897-2.

74)   Collins et al., High throughput toxicity screening and intracellular detection of nanomaterials. WIREs Nanomed Nanobiotechnol 2016. doi: 10.1002/wnan.1413.

75) Karlsson HL et al, 2015 Can the comet assay be used reliably to detect nanoparticle-induced genotoxicity? Mar;56(2):82-96. doi: 10.1002/em.21933. Epub 2014 Dec 8.

Leite et al., 2015. Gold nanoparticles do not induce myotube cytotoxicity but increase the susceptibility to cell death. Toxicology in Vitro 29 (2015) 819–827.

Tables

Table 1. Cell proliferation measured by ATP bioluminescence KIT, expressed by counts per minute.

Concentration	Nanoparticles				p value [b]
	Control	FeCoB	PAA-FeCoB	Cys-FeCoB	
0 µg ml^{-1}	1833.5* (1607.0 – 1898.0)				
0.1 µg ml^{-1}		1683.0 (1403.0 – 2050.0)	2043.0 (1086.0 – 2334.0)	1930.5 (927.0 – 2169.0)	n.s.
1 µg ml^{-1}		1456.0 (982.0 – 1797.0)	1641.0 (1367.0 – 2028.0)	1920.0 (1680.0 – 2646.0)	n.s.
10 µg ml^{-1}		1003.0 (737.0 – 1073.0)	1046.5 (937.0 – 1273.0)	1332.0 (1198.0 – 1971.0)	0.031
p value [a]		0.020	0.035	n.s.	

*Median and range; FeCoB: ferric cobalt boron; PAA-FeCoB: polyacrylic acid-coated ferric cobalt boron; cys-FeCoB: L-cysteine-coated ferric cobalt boron; ns: not significant. [a]p value within a NP type (kruskal wallis test), [b]p value within one concentration (kruskal wallis test), p≤0.05 was considered statistically significant

Table 2. Genotoxicity (single and double DNA strand breaks) measured by alkaline comet assay, expressed by tail intensity

Concentration	Nanoparticles				p value [b]
	Control	FeCoB	PAA-FeCoB	Cys-FeCoB	
0 µg ml^{-1}	4.49* (0.69 - 19.21)				
0.1 µg ml^{-1}		5.96 (2.89 - 7.66)	4.84 (2.77 – 10,71)	6.17 (3.20 – 26.61)	ns
1 µg ml^{-1}		3.86 (2.22 – 5.34)	8.66 (5.74 – 15.11)	10.76 (4.59 – 46.94)	0.032
10 µg ml^{-1}		18.59 (10.65 – 22.92)	41.51 (29.16 – 49.32)	41.71 (34.67 – 67.71)	0.012
p value [a]		0.016	0.002	0.011	

*Median and range; FeCoB: ferric cobalt boron; PAA-FeCoB: polyacrylic acid-coated ferric cobalt boron; cys-FeCoB: L-cysteine-coated ferric cobalt boron; n.s.: not significant. [a]p value within a NP type (kruskal wallis test), [b]p value within one concentration (kruskal wallis test), p≤0.05 was considered statistically significant

Table 3. Genotoxicity (micronuclei) measured by micronucleus test, expressed by the number of micronuclei per 500 cells

Concentration	Nanoparticles				p value [b]
	Control	FeCoB	PAA-FeCoB	Cys-FeCoB	
0 µg ml^{-1}	3.50 (1.65 – 7.09)				
0.1 µg ml^{-1}		2.24 (1.21 – 6.82)	2.00 (0.99 – 6.23)	2.00 (0.75 – 4.81)	n.s.
1 µg ml^{-1}		3.23 (1.00 – 7.94)	2.96 (1.49 – 7.99)	3.00 (1.47 – 5.22)	n.s.
10 µg ml^{-1}		5.5 (1.75 – 45,23)	5.00 (2.00 – 28.02)	4.00 (1.00 – 10.22)	n.s.
p value [a]		0.002	0.001	n.s.	

*Median and range; FeCoB: ferric cobalt boron; PAA-FeCoB: polyacrylic acid-coated ferric cobalt boron; cys-FeCoB: L-cysteine-coated ferric cobalt boron; n.s.: not significant. [a]p value within a NP type (kruskal wallis test), [b]p value within one concentration (kruskal wallis test), p≤0.05 was considered statistically significant
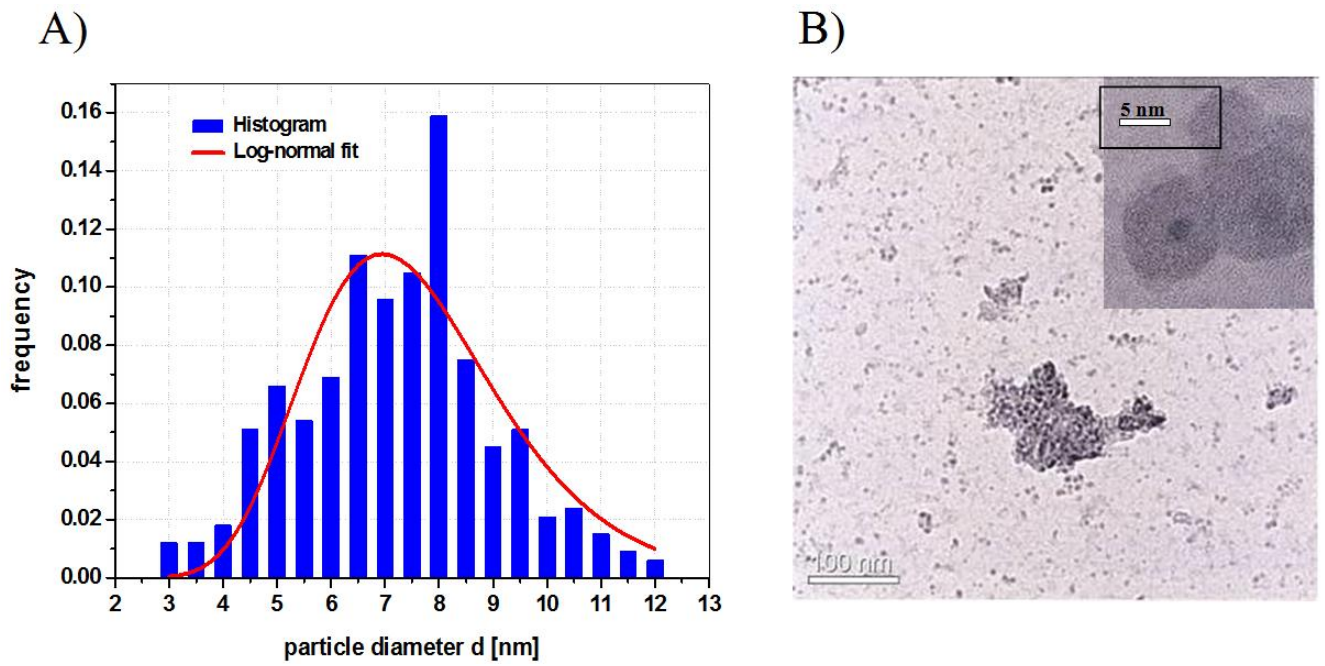
Figures

A)

B)

Figure 1: A) Histogram and log-normal-fit curve of particle diameters: <d> = 7.62 ± 1.93 nm. B) TEM-image of FeCoB-nanoparticles dried at a solid surface (TEM grid) with high resolution image in the upper right corner.
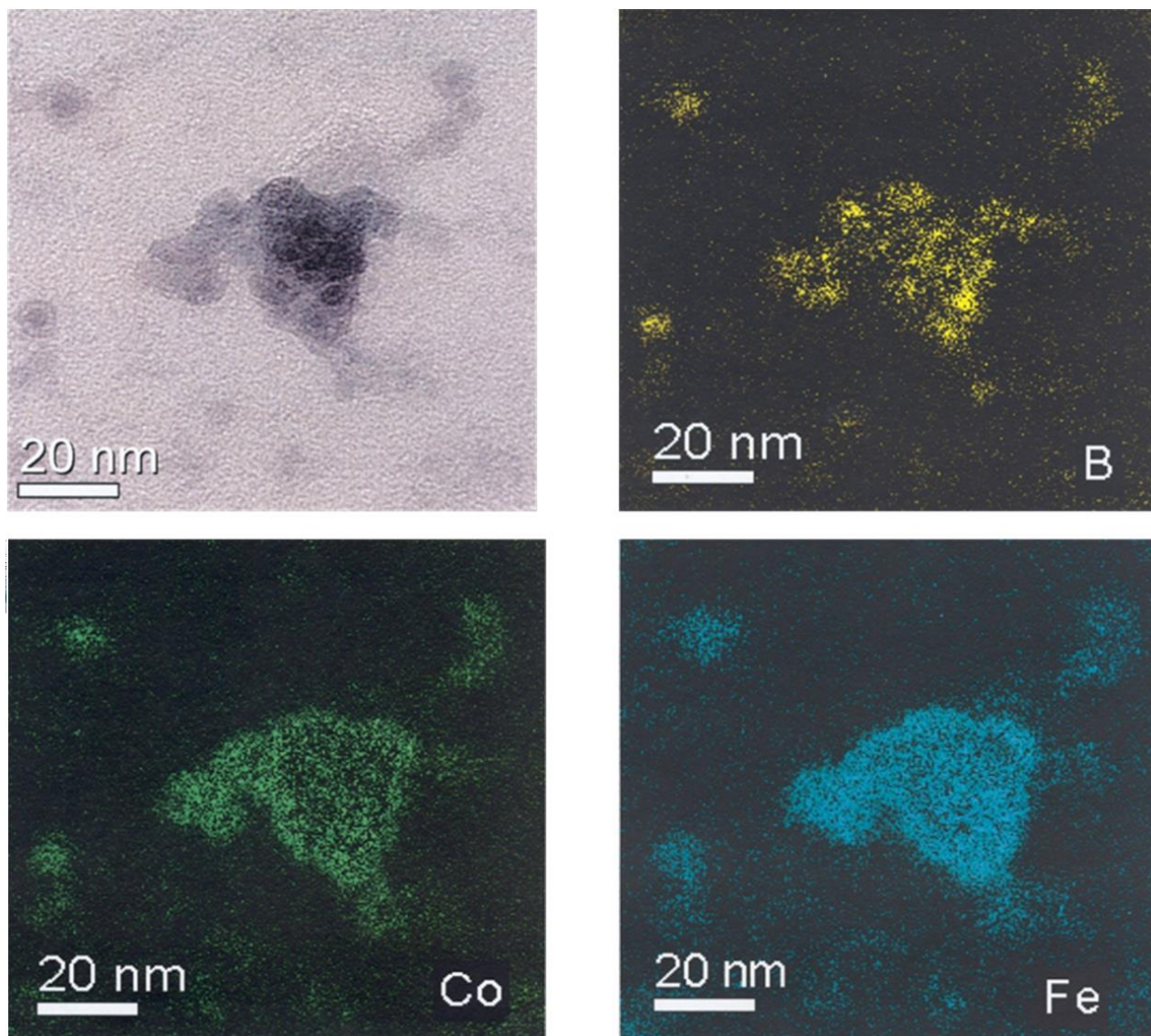
Figure 2: TEM image of FeCoB nanoparticles without energy filter and EELS-images of the same sector with energy filter setting specific for B, Co and Fe.